Material Characterization and Material Model Development for Simulating Elastomeric Parts in Diaphragm Pumps

Andreas Swienty[1]*, Robert Eberlein[2], Raphaël Thierrin[2], Nuno Dias Vidal de Castro[3]

[1]KNF Neuberger GmbH, 79112 Freiburg, Germany
Andreas.Swienty@knf.com

[2]Zurich University of Applied Science, Institute of Mechanical Modelling, 8400 Winterthur, Switzerland

[3]Zurich University of Applied Science, Institute of Materials and Process Engineering, 8400 Winterthur, Switzerland

* Corresponding Author

ABSTRACT

A diaphragm pump is a reciprocating positive displacement pump. It works according to the principle that a volume (working chamber) is periodically increased and decreased by a diaphragm. Due to this, a medium is sucked in and pushed out of the working chamber. Valves are used to prescribe the direction of flow and prevent back flow. The valves open and close automatically depending on the flow values or existing pressure differences. The diaphragm and, in many cases, the valves are made of a material which is capable of large reversible deformations such as elastomers (i. e. rubber). Such a material is necessary due to the diaphragm being stretched and compressed during its reciprocating movement. In addition, the flow domain is sealed off from the environment (this does not mean the sealing of the working chamber from the pressure or suction channels, but rather the prevention of leakage from the pump) by squeezing defined sealing surfaces on the diaphragm and the valves.

Numerical simulations with FEM are used to gain a deeper understanding of the movement, the strains and stresses that occur in the elastomeric part during operation. To achieve this, an adequate material model must first be created. A material model for elastomers differs substantially from a material model for steel, which in its simplest form consists only of a Young's modulus and a Poisson's ratio. Elastomeric materials show a behavior that is nonlinear elastic (hyperelastic) and time dependent (viscoelastic).

The aim of this paper is to present two methods for measuring the nonlinear stress-strain relationship of EPDM with large strains, which is also affected by temperature and the strain rate at which the material is stressed. Firstly, a hyperelastic characterization method at low strain rates with dynamical mechanical analysis is introduced. Secondly, an advanced method is described that enables the examination of hyperelastic material properties at high strain rates. Furthermore, two viscoelastic material models are calibrated on the base of these measurements, the first is a Prony series approach and the second uses a Bergstrom-Boyce model.

Finally, simulation results are compared with measurements. Measured stress-strain curves of a cyclic simple tension experiment are available for this purpose. This experiment is reproduced numerically. Comparing the results provides a first assessment of the material models.

1. INTRODUCTION

FEM simulations enable a deeper understanding of how elastic parts in a diaphragm pump work. The large elastic deformations of the components are of particular interest here. A material model is required for a reliable and correct simulation of the elastic components in a diaphragm pump, which are usually made of elastomeric materials. The material behavior of elastomers is generally described as hyperelastic with a time-dependent viscous component. In addition, these materials also show a temperature dependency as well as permanent deformations upon initial loading.

A review of different approaches for describing the material behavior of elastomers is presented in the next section. Then, appropriate material characterization is performed in order to fit and compare two models chosen with the knowledge provided in this review.

2. MATERIAL MODELS FOR ELASTOMERS

Purely elastic material behavior is described with nonlinear hyperelasticity models. Phenomena such as viscoelasticity, stress-softening or damage such as the Mullins effect (Mullins, 1969) are neglected. Only the pure nonlinear behavior with large strains is considered. The material is also assumed to be incompressible and isotropic. In the literature, these models are divided into three different types, all of which are a description of the strain-energy-density. Mooney (1940), Rivlin (1948) and Ogden (1972) developed phenomenological models. Yeoh (1990) and Gent (1996) derived models based on measurements. The last type of models is physics-based. Models like the 8-chain model by Arruda and Boyce (1993), as well as the neo-Hookean model by Treloar (1943) and Rivlin (1948) belong to this category.

The few material parameters that are present in all the mentioned models can be determined by tensile tests. In the frequently cited source Treloar (1944), uniaxial tension, pure shear and biaxial tension tests are carried out. This set of experiments remains used and recommended in more recent publications as well (Gent, 2012, Bergström, 2015 and Eberlein, 2019). Material models with parameters that are only determined by a single test, such as uniaxial tension, show good agreement with the respective test. However, the models fail most of the time when predicting other forms of deformation, especially if the material show a strong dependence on the second invariant of the right Cauchy-Green tensor.

Markmann and Verron (2006) examine 20 hyperelastic material models of the three types presented and evaluate how well they can reproduce different loading conditions. They describe that the Ogden model (Ogden, 1972) was able to reproduce all loading conditions well. However, they also note that models with 6 parameters require more effort to determine their right value. The Gent (1996) model with fewer parameters also shows good agreement with corresponding experimental data with small deviations when predicting the biaxial test. For strains up to 150 %, they recommend the Mooney-Rivlin or neo-Hookean model for their efficiency.

Linear viscoelastic material models describe the time-dependent material behavior. This is, for example, a stress relief of a tensile specimen at constant strain (relaxation) or creep of the material at constant load. To understand the material model, a model analogy consisting of a spring with the stiffness E and a damper with the damping constant η can be used. In the following, only calculations for the relaxation are presented. Figure 1 shows a Maxwell element in the dashed box with spring and damper in series. The procedure is very similar for creep. It is also possible to carry out a conversion from relaxation to creep and vice versa. Further explanations can be found in the literature which is mentioned at the end of this section. Both elements are connected in series and are subjected to strain. The stress, however, is the same in both elements. This results in the following differential equation:

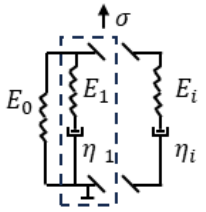

Figure 1: Maxwell model and the extension with several spring-damper elements

$$\dot{\epsilon} = \frac{1}{E}\dot{\sigma} + \frac{1}{\eta}\sigma. \tag{1}$$

The following analytical solution can be found using the exponential function as the starting function:

$$\sigma(t) = \epsilon(0)Ee^{-\frac{t}{\tau}} \text{ with } \tau = \frac{\eta}{E}. \tag{2}$$

The first parameter on the right-hand side represents a constant initial strain at time 0. A generalized Maxwell model is used for an extended description. For this purpose, several spring-damper elements are connected in parallel (Figure 1). In the first branch, however, only one spring with the stiffness E_0 without damper is used to represent the time-independent material behavior. Equation 2 then takes the form:

$$\sigma(t) = E_0\epsilon(0) + \sum_{i=1}^{N} \epsilon(0)E_i e^{-\frac{t}{\tau_i}}. \tag{3}$$

By applying Prony series to this approach, an arbitrary function for the relaxation can be defined. So far, only one strain at time $t = 0$ is considered. An integral is introduced for arbitrary and continuous strains:

$$\sigma(t) = E_0\epsilon(t) + \sum_{i=1}^{N} \int_0^t E_i e^{-\frac{t-s}{\tau_i}} \frac{\partial\epsilon(s)}{\partial s} ds. \tag{4}$$

Equation 4 can also be stated in the frequency domain instead of the time domain. The excitation is now a sinusoidal strain $\epsilon(t) = \epsilon_0 + \Delta\epsilon\sin(\omega t)$. Inserting this into 4 with $N = 1$ results in:

$$\sigma(t) = E_0\epsilon_0 + E_0\Delta\epsilon\sin(\omega t) + \omega\Delta\epsilon E_1 \int_0^t e^{-\frac{E_1(t-s)}{\eta_1}} \cos\omega t \, ds. \tag{5}$$

By rearranging the equation and calculating the integral, it can now be written as follows:

$$\sigma(t) = E_0\epsilon_0 + \Delta\epsilon \left\{ \left(E_0 + \frac{\omega^2 E_1}{\omega^2 + \left(E_1/\eta_1\right)^2} \right) \sin\omega t \; + \frac{\omega E_1^2/\eta_1}{\omega^2 + \left(E_1/\eta_1\right)^2} \cos\omega t \right\} \tag{6}$$

In the linear viscoelastic model, the stresses due to strains at further time steps $t > 0$ just add up. This is known as the Boltzmann superposition. It can also be seen in 2 and 3 that the shape of the stress relaxation is qualitatively the same due to the exponential function. Only a scaling with the occurring strains is carried out. A linear viscoelastic model therefore does not necessarily have a linear stress-strain relationship. Instead, the linearity relates to the superposition and the scalability. A detailed description of this theory can be found in the books by Findley, Lai and Onaran (1976) or Christensen (1982).

If the assumption of superposition and scalability does not apply to the material, the viscoelastic material behavior is not linear. Nonlinear viscoelasticity is discussed in detail by Noll (1958) and Truesdell and Noll (1965). Wineman (2009) summarizes the progress in modeling nonlinear viscoelastic materials, while Ward and Sweeney (2013) divide the nonlinear models into three approaches: engineering approach, rheological approach and molecular approach. In the engineering approach, empirical models are derived from a manageable number of measurements. The applicability and transfer of these approaches are limited. The rheological approach contains most of the nonlinear models. Schapery's model (1969) is widely used. A model by Leaderman (1943), later modified by Findley and Lai (1967), is also mentioned in the literature. Pipkin and Rogers (1968) then present a more general model. All four models describe the nonlinear viscoelasticity with a single integral, like the approach for the linear viscoelastic models in (4). Here, however, the function for the relaxation or creep is dependent on time and the strains or stresses. The last of the class of single integral models is the BKZ model by Bernstein, Kearsley and Zapas (1963). They primarily developed a model for elastic fluids which can also be applied to solids. Finally, the more complex and therefore less used multiple-integral model by Green and Rivlin (1957) is mentioned. In the molecular approach, Halsey et al. (1945) develop a model based on the movement of molecular chains. In addition, they defined an activation energy and an activation volume for the time-dependent behavior. The damper in the model analogy is only active when a threshold is exceeded.

One of the latest approaches of modeling the time-dependent material behavior of elastomers is made by Bergstrom and Boyce (1998). Their model is micromechanically inspired from the relaxation of a single entangled chain in a polymer gel matrix. This model can also be counted among the nonlinear viscoelastic models, but it does not use an integral for calculating the time dependent stress or strain behavior. This model consistently uses the 8-chain model of Arruda and Boyce (1993) for the elastic material behavior. For determining the parameters of such models, experimental stress and strain curves at different strain rates, especially at high strain rates and large strains, are necessary. Such strain rates often exceed the capabilities of standard testing machines. Testing at high strain rates is commonly done using a Kolsky or Split-Hopkinson Bar (SHPB, Miyambo et al., 2023). However, the SHPB requires substantial adjustments for polymers and elastomers (Yoon et al., 2016 and Cheng et al., 1999) and may suffer from

a high signal noise and a low transmitted signal (Brown, 2018). An increasingly popular alternative method for performing mechanical test at high strains on softer materials involves a so-called Drop Tower (typically >50 /s up to 500 /s in tension and 2'000 /s in compression). The Drop Tower offers a simpler approach better suited for testing softer materials. Its operating mechanism consists of a heavy sled falling along two vertical pillars, either equipped with a punch and impacting a sample (compression) or dragging a part of the sample holder after impact to pull on the sample (tension). A more detailed description of this method is provided by Teller (2019).

In addition to the time-dependent material behavior, the temperature-dependent behavior is also described in the literature (Gent 2001). Considering the spring-damper model analogy it is understandable that the viscosity of the damper naturally also depends on the temperature. The glass transition temperature is a characteristic parameter for elastomers. Below the glass transition temperature ($T << T_g$), elastomers are glassy, brittle and exhibit a relatively high stiffness, while at temperatures above the glass transition temperature ($T >> T_g$) elastomers show a rubber-like behavior which is characterized by a much lower stiffness. If the damper from the model analogy is used again, it quickly becomes clear that temperature and time are superimposed in the viscoelastic behavior. Several authors, among which Gent (2001) and Ferry (1980) also describe this at the molecular level. The correlation of time and temperature is described by the time-temperature-superposition principle. When all relaxation functions have the same dependency on time, this also means that the shape of the relaxation functions is identical for all temperatures. Therefore, the material is considered as a thermorheological simple material. This allows measurements of the material behavior at different temperatures over a limited range of strain rates to be combined into an overall curve at a reference temperature to obtain a statement about the material behavior over a wide range of strain rates. Particularly low strain rates sometimes take a very long time to converge into a result. On the other hand, particularly high strain rates can sometimes only be measured with great technical effort. The shift of the master curve to a temperature other than the reference temperature is described for elastomers by the Williams-Landel-Ferry (WLF) function.

In the following, experimental approaches for the characterization of EPDM (ethylene propylene diene monomer rubber) are presented. Common to all approaches is, that the hyperelastic material properties are first determined. This is based on the literature and the quasi-static measurements described by Treloar (1944). Two types of measurements are then conducted to determine the viscoelastic material properties. First, a standardized dynamic mechanical analysis (DMA) is performed assuming the time-temperature-superposition principle. This is a standard test for elastomers and is described by Gent (2001) and Kraus et al. (2017). In addition, a drop tower is used to investigate high strain rates and large strains. The obtained experimental data is then used to calculate parameters for the numerical material models. In the simulation program Marc, a variety of hyperelastic material models can be selected. In this article, the Mooney-Rivlin model is used for moderate strains, as recommended by Markmann and Verron (2006). In addition, a linear viscoelastic material model capable of large deformations is used for the time-dependent material behavior. A model by Simo (1987) is implemented in Marc for this purpose. The parameters of the Prony series are determined from the DMA. Finally, the model parameters of the nonlinear viscoelastic model by Bergstrom and Boyce (1998) in conjunction with the hyperelastic model by Arruda and Boyce (1993) are determined using the measurements from the drop tower. The same approach was adopted by Eberlein et al. (2019) with thermoplastic polyurethanes using a Three-Network-Model, an extension of the Bergstrom Model (Bergstrom and Bischoff, 2010). Bergstrom (2015) also states that the parameters of this model can be determined with tests at high strain rates.

3. MEASUREMENTS

This section presents the experimental procedures used to obtain the data necessary to the calibration of the chosen models. The experimental conditions to adequately characterize the viscoelastic behavior of the material must be similar to the working conditions of the diaphragm pump. The pump operates at temperatures around 80 °C and strain rates of around 50 /s are experienced by the diaphragm, which is replicated in the high strain rate measurements. The quasi-static measurements for the hyperelastic part of the model are measured at room temperature. The influence of higher temperatures and strain rates is taken into account by the DMA.

Data processing applied to raw data includes the isolation of the evaluation cycle for cyclical tests (i.e. discarding the pre-conditioning for evaluation), as well as smoothing the raw data, eliminating experimental artifacts (Toe-In) and homogenizing the number of data points for each measurement.

3.1 Quasi-static mechanical characterization of EPDM

The main experimental parameters and sample characteristics are presented in Table 1. The quasi-static experiments are performed with a custom-made biaxial testing machine, after principles shown in Eberlein and Holenstein (2018). The force is measured by loadcells on each arm and the strain is measured with a video-extensometer that tracks appropriately drawn contrast-marks. The testing for all three loading modes (Figure 2) is performed as a path-controlled cycle with monotonous loading followed by a holding period and then monotonous unloading. This evaluation cycle is preceded by three identical cycles to account for the Mullins Effect (Mullins, 1969). This is necessary when the aim is to characterize a part in use, where the loading history of the material must be considered.

Table 1: Experimental parameters for the mechanical characterization of EPDM (quasi-static and high strain rate)

Experimental parameters	*Uniaxial tension*	*Pure shear*	*Biaxial tension*	*High strain rate uniaxial tension*	*High strain rate uniaxial compression*
N° samples	--------- 3 ---------			---------	6 ---------
Shape	Dogbone (ISO 37 Type 2)	Rectangular (100 mm x 40 mm)	Square (100 mm x 100 mm)	Dogbone (ISO 37 type 3)	Cylinder (Stack of 6 discs with d=6mm)
Thickness	---------- 1mm ----------				
Strain rate	<0.005 /s	<0.005 /s	<0.005 /s	3x 13 /s ; 3x 55 /s	3x 36 /s ; 3x 47 /s
Target strain	35 %	35 %	35 %	na	na
Loading scheme	Load - hold 180s - unload			Single loading ramp until failure	

Figure 2: Mechanical testing: quasi-static testing configurations - a) uniaxial tension, b) equibiaxial tension and c) pure shear

3.2 Mechanical characterization of EPDM at high strain rates

High strain rate and large strain mechanical testing is performed using a Drop Tower. Figure 3 shows the Drop Tower in two different configurations for tension and compression experiments. The force is captured by a loadcell. Displacement and strain are calculated by post processing using a DIC (digital image correlation) routine on images recorded by a highspeed camera. To this end, a speckle pattern is applied onto the tension samples, whereas no markings are required for compression samples (the displacement of the punch is tracked upon contact with the sample). The material is tested in uniaxial tension and compression. Before testing, a pre-conditioning routine is applied to the samples analogous to the quasi-static testing. The pre-conditioning is performed quasi-statically using a universal testing machine. The experiments are performed for two target strain rates (10 /s and 50 /s). On the Drop Tower, the strain rate is set by adjusting the falling height of the sled. This is especially challenging for strain rates at the lower end of the Drop Tower's spectrum applied to small samples, as the falling height must be set in relation to the sample height (compression) or length (tension). Thus, the target strain rate of 10 /s could not be achieved for compression tests.

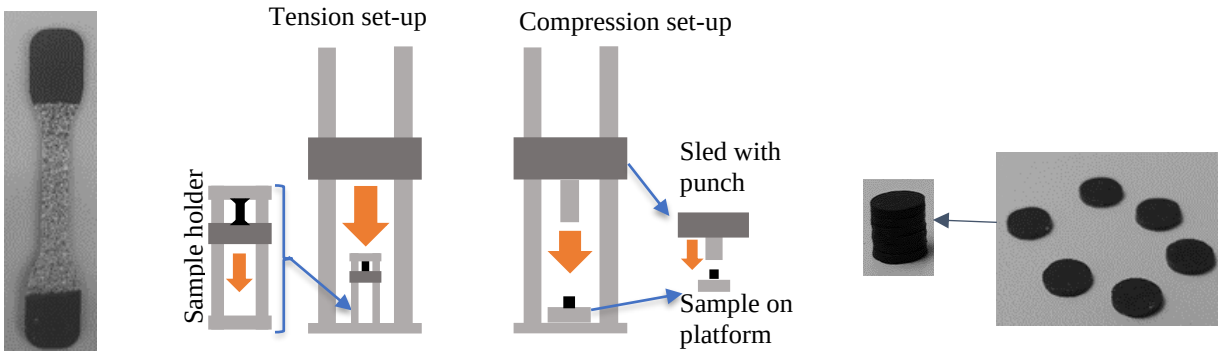

Figure 3: Schematic representation of the Drop Tower and the set-ups for tension and compression. Darker grey elements with a wide arrow indicate the mobile components. Samples for the respective configurations are presented right and left.

3.3 Dynamic Mechanical Analysis

The dynamic-mechanical analysis was carried out based on ISO 6721-7 (forced vibration, non-resonant) under dynamic torsional stress. The MCR 702 test device was used for the tests. The tests were carried out in a measuring frequency range of 0.1 Hz to 10 Hz, with a constant strain of 0.05 % in a temperature range of -100°C to 100 °C. The heating rate was 0.5 K/min. Beforehand, it was also assessed whether the material behaves like a linear viscoelastic material within the strain range used. For each 1 K increase in the measurement sequence, the entire frequency range was tested. As a result of the investigations, the real and loss components G′ and G'' of the complex shear modulus G^* were determined as a function of temperature and frequency. Rectangular strips with a width of 10 mm were punched out for the measurements. A sample length of 44 mm was used for testing. After subtracting the fixtures, this results in a measuring length of 30 mm.

3. RESULTS AND DATA EVALUATION

An application in the simulation program MARC is used to fit the material model from the measurement results. After the measurement data is imported into the simulation program, the unknown model parameters are then determined by minimizing the least squares error between the computed response and the measurements using the differential evolution method (Storn, R. and Price, K., 1997). In the hyperelastic material model, the stress-strain behavior is obtained by deriving the strain-energy-density function with respect to the stretches or the invariants of the right Cauchy-Green tensor. As already described, the Mooney-Rivlin model has two parameters denoted by C_{01} and C_{10}. The material model is calibrated by adjusting the two parameters until the deviation between the experimental data and curves calculated from the material model is minimized. Figure 4 shows the measurement results and the calculated response of the material model. It is easy to see that the curves lie well on top of each other. The least squares error is 1 %. The maximum absolute error of a single point in the ST test is 40 %. This can be found at an elongation < 10 %. For strains above 10 %, the absolute error decreases to 5 %. Nevertheless, the fit of the measurement data is acceptable and adequate values for C_{01} and C_{10} are obtained.

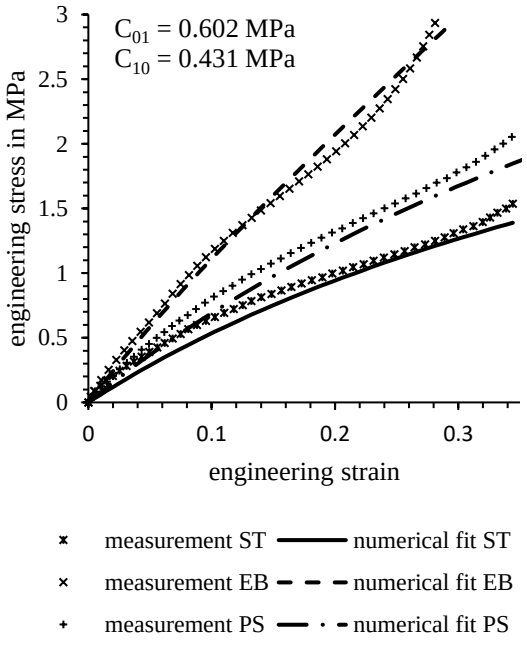

Figure 4: Comparison of measured data (dotted line) and response of the material model (solid line) for simple tension (ST), pure shear (PS) and equal biaxial extension (EB)

The pre-factors in Equation 6 are referred to as the storage modulus $G'(\omega)$ and loss modulus $G''(\omega)$:

$$G'(\omega) = E_0 + \frac{\omega^2 E_1}{\omega^2 + \left({}^{E_1}/_{\eta}\right)^2} \text{ and } G''(\omega) = \frac{\omega {}^{E_1^2}/_{\eta}}{\omega^2 + \left({}^{E_1}/_{\eta}\right)^2}. \quad (7)$$

$G'(\omega)$ describes the elastic material property and $G''(\omega)$ describes the damping. It is convenient to expand the storage and loss moduli with Prony series. These parameters can then be calibrated to DMA measurements as it was done above for the hyperelastic model. However, only small strains can be examined with the DMA. 22 terms are used for the Prony series, as the master curve of the measurements extends over 22 decades (see Kraus et al., 2017). This means that 22 E_i and τ_i parameters must be determined. For assembling the master curve, -55 °C is selected as the reference temperature, as this is where the greatest change in the storage modulus occurs. Figure 5 shows the storage and loss master curves, which are assembled from the measured data with the frequency and temperature sweep. The stiffness values in the lower and upper range are similar to the measurements of Qu et al. (2017). In addition, the graph shows the master curves from the Prony series approximation of the measured data. The least squares error is 0.7 %. The short-term stiffness with 1100 MPa is in the same range as the measurement results with 1150 MPa at high frequencies. The long-term stiffness with 5 MPa is also in the range of the measurements with 5.5 MPa. The largest deviation is in the peak of the loss modulus. Here the absolute deviation is 13 %. Compared to other authors such as Kraus et al. (2017), this is a good numerical approximation of DMA measurements. Merging this Prony series with the hyperelastic Mooney-Rivlin model allows the formulation of a linear viscoelastic model for large strains.

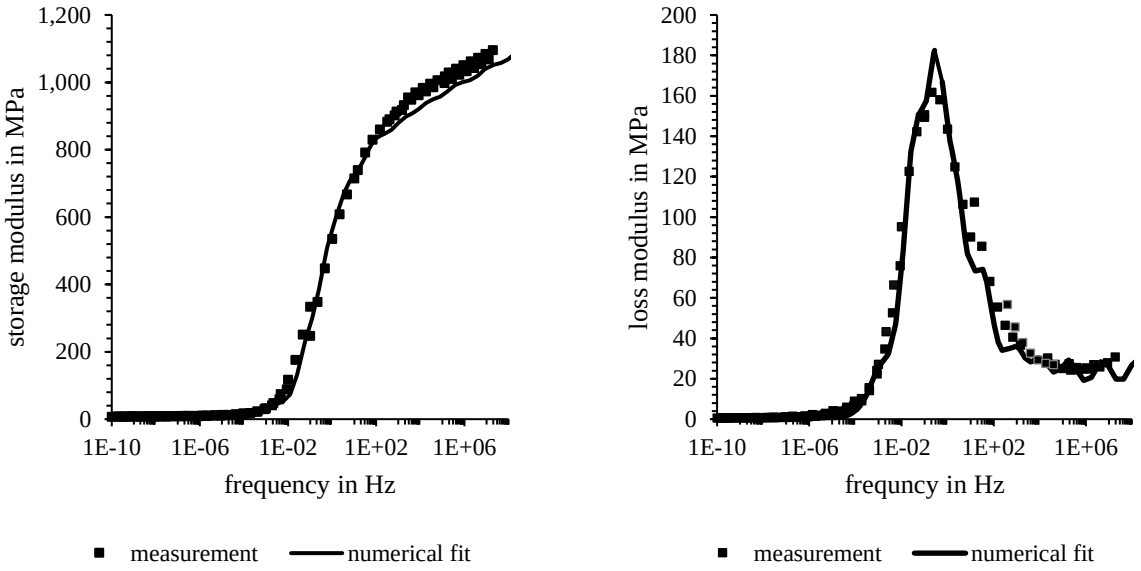

Figure 5: Comparison of the master curves from measurement and material model (storage modulus left and loss modulus right)

The measurements from the drop tower are used to determine the model parameters for the Bergstrom Boyce model. Here too, the first step is to import the tension and compression measurement curves at two strain rates into the simulation program. For this model, the hyperelastic component is determined by two parameters of the Arruda-Boyce formulation and five parameters determine the viscoelastic behavior (two for the nonlinear spring and three for the nonlinear damper). All seven parameters are calculated in a joint fitting process. The least squares error is 0.44 % and is therefore the lowest value achieved in this work. Figure 6 compares the measurement and simulation results. The difference between the high and low strain rate measurements is small. This is due to the high temperature of the measurement. In the compression, the curves are almost congruent. It is noticeable that the numerical fit reproduces the measurement results very well. The slightly different slope of the curves at high and low strain rate is also reproduced.

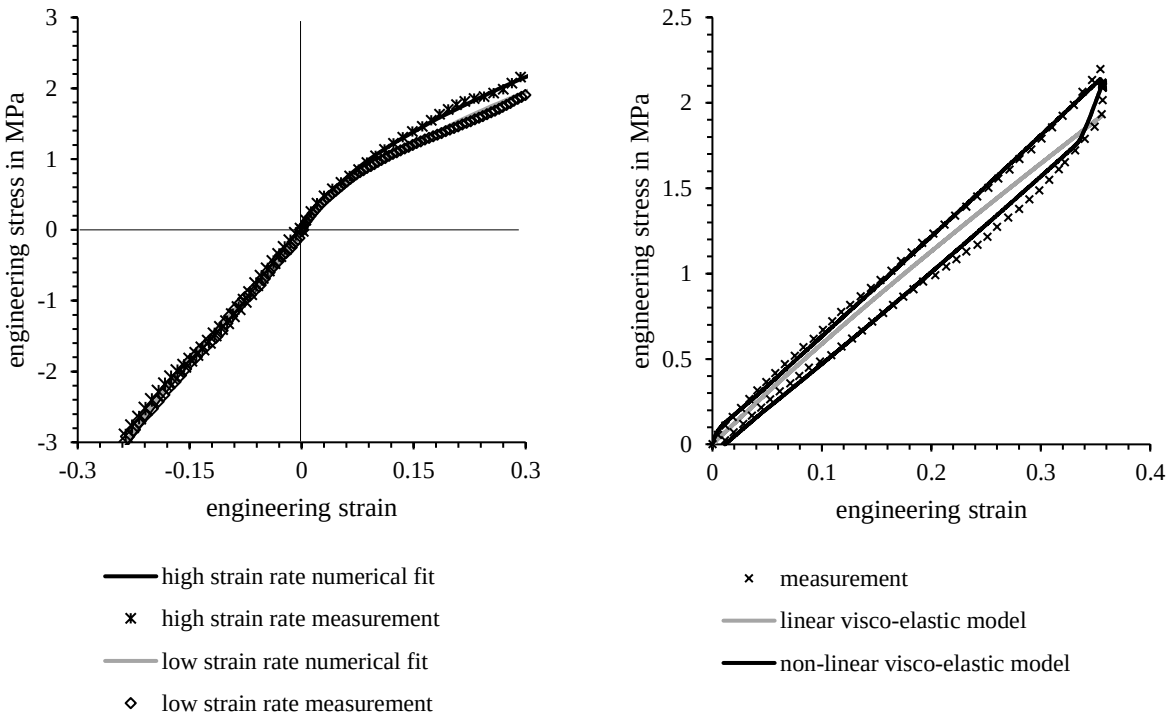

Figure 6*:* Comparison of measurement data from the drop tower and response of the material model (left) as well as comparison of the simulation results of the single-element test with cyclic simple tension measurement data (right)

A linear viscoelastic and a nonlinear viscoelastic model are now calibrated for large strains. Both models match well with the respective experiments. Finally, a simple simulation is used to investigate how well the models work. A stress-strain curve from cyclic simple tension measurements is available. A sample is stretched at a strain rate of 0.43 % per second up to 35 %, then held for 180 s (the relaxation is clearly visible in Figure 6 right) and finally released again at 0.43 % per second. This measurement is reproduced in a simulation. For simplicity, only one element is used for this, which is pulled axially. Figure 7 shows how the element is fixed and where the tensile force is applied. Figure 6 compares the measurement and simulation results. It is easy to observe that both models are capable of reproducing the material behavior in the loading phase of the cycle. However, only the nonlinear viscoelastic model is able to reproduce the stress relaxation in the holding phase and the material behavior in the unloading phase. In the linear viscoelastic model, the stress-strain curves follow the same path during stretching and releasing. In this model, stress relaxation takes place on a much smaller time scale. Therefore, no stress relaxation can be recognized in the holding phase, as the stress falls directly to the long-term value due to the low strain rate while stretching.

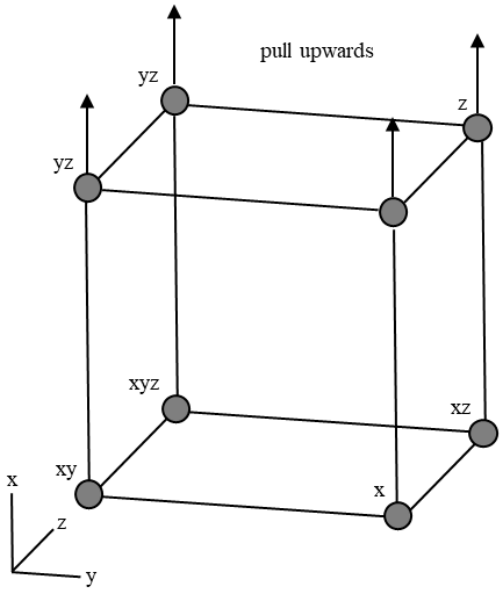

Figure 7: One element test

CONCLUSIONS

This work offers a glimpse of the complexity and diversity of material models suitable for describing elastomers. The development of such material models began in the middle of the last century and is still ongoing. Based on previous research in this field, two approaches were chosen. A linear viscoelastic model with Prony series in combination with a hyperelastic model as a well-established method and a nonlinear Bergstrom-Boyce model as one of the latest developments in modeling viscoelastic material behavior were selected. Both models are implemented in the simulation software used for this work. Suitable measurements were described and carried out to determine parameters for both models. The calibration of the material models from the measurements worked reliably for each model and the least squares error is low (< 1 %) for all calculations. The comparison of measurement and material model response are in good agreement. However, checking the functionality of the material models when reproducing a cyclic tensile test shows that only the nonlinear viscoelastic model is capable of adequately reproducing the stress-strain behavior. A definitive assessment of which model will be used for further simulations of diaphragm movement cannot yet be made. For this purpose, a test rig will be set up in a future study to measure the forces during a stroke movement of a diaphragm pump. This test will then be reproduced numerically. The different material models will be assessed again in a setting closer to their final application. These more complex simulations can then be used to assess potential differences in numerical stability and computational efficiency between the material models.

NOMENCLATURE

C_{01}, C_{10}	Parameter material model	N/m^2	σ	Stress	N/m^2
E	Stiffness	N/m^2	$\dot{\sigma}$	Stress rate	$N/(m^2\ s)$
ϵ	Strain	$-$	s	Time	s
$\dot{\epsilon}$	Strain rate	s^{-1}	t	Time	s
η	Damping rate	$N\ s/m^2$	T	Temperature	$°C$
G', G''	Storage, Loss Modulus	N/m^2	xyz	Coordinates	m
G^*	Complex Modulus	N/m^2	ω	Frequency	s^{-1}

REFERENCES

Arruda, E. and Boyce, M. C. (1993). A three-dimensional constitutive model for the large stretch behavior of rubber elastic materials. *Journal of the Mechanics and Physics of Solids, 41*(2), 389-412.

Bergstrom, J. S. (2015). *Mechanics of Solid Polymers, Theory and Computational Modeling*. William Andrew, Plastic Design Library. Elsevier.

Bergstrom, J. S., Anderson, D., Quinn, D., Schmitt, E., Brown, S. & Chow, S. (2014). High Strain Rate Testing and Modeling of Polymers for impact Simulations. *13th International LS-DYNA Users conference*.

Bergstrom, J. S. & Bischoff, J. E. (2010). An Advanced Thermomechanical Model for UHMWPE. *International Journal of Structural Changes in Solids, 2*(1), 31-39.

Bergstrom, J. S. & Boyce, M. C. (1998). Constitutive modeling of the large strain time-dependent behavior of elastomers. *Journal of the Mechanics and Physics of Solids, 46*, 931-954.

Bernstein, B., Kearsley, E. A. & Zapas, L. J. (1963). A Study of Stress Relaxation with Finite Strain. *Transactions of The Society of Rheology, 7*, 391-410.

Brown, S., Teller, S., Bergstrom, S. & Oliver, M. (2018). Techniques to Measure Impact Properties of Polymers. *SPE (Society of Plastics Engineers) ANTEC 2018, 1*, 100-104.

Christensen, R. M. (1982). *Theory of Viscoelasticity - An Introduction* (2nd Edition). New York: Academic Press.

Cheng, W., Zhang, B. & Forrestal, M. J. (1999). A Split Hopkinson Bar Technique for Low-impedance Materials. *Experimental Mechanics, 39*, 81-85.

Eberlein, R. & Holenstein, S. (2018). Efficient Material Parameter calibration of elastomer Specimen in uniaxial Tension, planar Shear and equibiaxial Tension. *KGK, 7-8*, 36-40.

Eberlein, R., Pasieka, L. & Rizos, D. (2019). Validation of Advanced Constitutive Models for Accurate FE Modeling of TPU. *Advanced Materials Letters, 10*(12), 893-898.

Ferry, D. J. (1980). *Viscoelastic Properties of Polymers* (3rd Edition). New York: Wiley.

Findley, W. N. & Lai, J. S. Y. (1967). A Modified Superposition Principle Applied to Creep of Nonlinear Viscoelastic Material under Abrupt Change in State of Combined Stress. *Transactions of the Society Rheology, 11*, 361-380.

Findley, W. N., Lai, J. S. & Onaran, K. (1976). *Creep and Relaxation of Nonlinear Viscoelastic Materials*. Amsterdam: North-Holland.

Gent, A. N. (1996). A New Constitutive Relation for Rubber. *Rubber Chemistry and Technology*, *69*(1), 59-61.

Gent, A. N. (2001). *Engineering with rubber*. Munich: Carl Hanser Verlag.

Green, A.E. & Rivlin, R.S. (1957). The mechanics of non-linear materials with memory - Part I. *Archive for Rational Mechanics and Analysis*, *1*, 1-21.

Halsey, G., White, H.J. & Eyring, H. (1945). Mechanical Properties of Textiles, I. *Textile Research Journal, 15*(9), 295-311.

Kraus, M. A., Schuster, M., Kuntsche, J., Siebert, G. & Schneider, J. (2017). Parameter identification methods for visco- and hyperelastic material models. *Glass Structures and Engineering, 2*, 147-167.

Leaderman, H. (1943). *Elastic and creep properties of filamentous materials and other high polymers*. Washington, D.C.: The Textile Foundation.

Marckmann, G. & Verron, E. (2006). Comparison of hyperelastic models for rubber-like materials. *Rubber Chemistry and Technology*, *79*(5), 835-858.

Miyambo, M. E., Kallon, D., Pandelani, T. & Reinecke, J. D. (2023). Review of the development of the split Hopkinson pressure bar. *33rd CIRP Design Conference*, *119*, 800-808.

Mooney, M. J. (1940). A Theory of Large Elastic Deformation. *Journal of Applied Physics, 11*, 582-592.

Mullins, L. Softening of rubber by deformation. *Rubber Chemistry and Technology*, *42*, 339-362.

Noll, W. A. (1958). Mathematical theory of the mechanical behavior of continuous media. *Archive for Rational Mechanics and Analysis*, *2*, 197-226.

Ogden, R. W. (1972). Large Deformation Isotropic Elasticity - On the Correlation of Theory and Experiment for Incompressible Rubberlike Solids. *Proceedings of the Royal Society of London. Series A, 326*, 565-584.

Pipkin, A. C. & Rogers, T. G. (1968). A non-linear integral representation for viscoelastic behavior. *Journal of the Mechanics and Physics of Solids, 16*, 59-72.

Qu, M., Ma, Y., Li, C. & Shi, X. (2017). Investigation of the properties of polynorbornene rubber/EPDM blends. *Journal of Elastomers & Plastics*, *49*(7), 560-573.

Rivlin, R. S. (1948). Large elastic deformations of isotropic materials. I. Fundamental concepts. *Philosophical Transactions of the Royal Society of London. Series A, Mathematical and Physical Sciences, 240*, 459-490.

Rivlin, R. S. (1948). Large Elastic Deformations Isotropic Materials. IV. Further Developments of the General Theory. *Philosophical Transactions of the Royal Society Series A, Mathematical and Physical Sciences*, 241(835), 379-397.

Schapery, R. A. (1969). On the characterization of nonlinear viscoelastic materials. *Polymer Engineering & Science, 9*, 295-310.

Simo, J. (1987). On a fully three-dimensional finite-strain viscoelastic damage model: fomulation and computational aspects. *Computer Methods in Applied Mechanics and Engineering*, *60*, 153-163.

Storn, R. & Price, K. (1997). Differential Evolution—A Simple and Efficient Heuristic for Global Optimization over Continuous Spaces. *Journal of Global Optimization*, *11*, 341-359.

Teller, S. (2019). High strain rate testing of elastomers and thermoplastic elastomers. *RubberWorld*, 259(4), 40-43.

Treloar, L. R. G. (1943). The elasticity of a network of long-chain molecules-II. *Transactions of the Faraday Society, 39*, 241-246.

Treloar, L. R. G. (1944). Stress-strain data for vulcanized rubber under various types of deformation. *Transactions of the Faraday Society*, *40*, 59-70.

Truesdell, C. and Noll, W. (1965). *The Non-linear Field Theories of Mechanics*. (3rd Edition). Berlin: Springer.

Ward, I. M. & Sweeney, J. (2013). *Mechanical Properties of Solid Polymers*. (3rd Edition). John Wiley & Sons, Ltd.

Williams, M. L., Landel, R. F. & Ferry, J. D. (1955). The Temperature Dependence of Relaxation Mechanisms in Amorphous Polymers and Other Glass-forming Liquids. *Journal of the American Chemical Society*, *77*(14), 3701-3707.

Wineman, A. S. & Rajagopal, K. R. (2000). *Mechanical Response of Polymers, An Introduction*. Cambridge: Cambridge University Press

Wineman, A. (2009). Nonlinear Viscoelastic Solids--A Review, *Mathematics and Mechanics of Solids*. 14, 300-366.

Yeoh, O. H. (1990). Characterization of Elastic Properties of Carbon-Black-Filled Rubber Vulcanizates. *Rubber Chemistry and Technology*, *63*(5), 792-805.

Yoon, S.-H., Winters, M. & Siviour, C.R. (2016) High Strain rate Tensile Characterization of EPDM Rubber Using Non-Equilibrium Loading and the Virtual Fields Method. *Experimental Mechanics, 56*, 25-35.